Instantaneous diffusion effect on spin-echo decay: Experimental investigation by spectral selective excitation

S. Agnello, R. Boscaino, M. Cannas,* and F. M. Gelardi
Dipartimento di Scienze Fisiche ed Astronomiche dell'Università and Istituto Nazionale per le Fisica della Materia, Via Archirafi 36, I-90123 Palermo, Italy
(Received 3 April 2001; published 16 October 2001)

The influence of the instantaneous diffusion process on spin-echo decay of E'_γ centers in gamma irradiated silica is experimentally probed by spectral selective excitation within their inhomogeneous resonance line. Our results evidence the different effectiveness of this dephasing mechanism on varying the resonance field, manifesting itself by a faster decay of the echo signal when generated by spin packets located in the central part of the spectrum. It is shown that the dependence of the instantaneous diffusion rate on the spectral position of echo-active spins reproduces the shape of the E'_γ centers resonance spectrum. These features are discussed in the framework of theoretical models concerning the transversal spin relaxation in solid systems and point out the correlation between the instantaneous diffusion rate and the concentration of echo-active spins located within a spectral bandwidth of the order of the Rabi frequency.

DOI: 10.1103/PhysRevB.64.174423 PACS number(s): 76.60.Lz, 76.90.+d, 42.50.Md

I. INTRODUCTION

Among the electron spin resonance (ESR) techniques, echo decay measurements have been proven to be one of the most useful tools to investigate the transversal relaxation mechanisms due to the spin-spin dipolar interaction.[1–3] In particular, much attention has been devoted to electron spin echo (ESE) experiments in solids.[2,4–11] In these systems, the inhomogeneous distribution $f(\omega)$ of the spin resonance frequencies is rather broad and the Rabi frequency χ induced by the driving field is usually much less than the width σ of $f(\omega)$. In this case, the echo signal is generated by the partial excitation of $f(\omega)$ and the spins are conveniently divided in two sets: the *A* spins (echoactive) that are directly excited by the radiation and the *B* spins that are the remainder of the system.[12] The distinction between the *A* and *B* spins, based on their spectral position within the inhomogeneous line, has been experimentally tested by frequency-domain measurements that evidenced the contribution of the echo active *A* spins located within a spectral bandwidth of the order of χ around the frequency of the driving field.[11,13]

The interactions of the *A* spins with each other and with the *B* spins contribute in a different way to the attenuation of the ESE signal, through the instantaneous diffusion (ID) and the spectral diffusion (SD) processes, respectively.[2,5–11,14–17] The SD is associated with the randomization effect of the precession phases of *A* spins caused by their interaction with the *B* spins, the latter changing their orientation both by spin-lattice interaction and by mutual spin flip-flops. On the other hand, the ID arises from the modulation of the *A* spins frequencies resulting from the spin flips induced by the driving microwave field and it is effective only during the second refocussing pulse. So, ID is a fingerprint of the dipolar interaction strength among the excited *A* spins and it is related to the total spin concentration.[5] Up to now, the ID contribution to the echo decay dynamics has been observed mainly in experiments in which its effectiveness was externally controlled by varying either the width or the amplitude of the second pulse.[2,5–8,10,11,18] Poor consideration has been given to the dependence of ID on the spectral position of *A* spins within the inhomogeneous line $f(\omega)$. To this aim, we report here a study on both ESE time-decay curves and field swept ESE spectra performed on a spin system of E'_γ centers[19] in vitreous silica, in which ID is the main contribution to the relaxation mechanisms that affect the echo decay. This condition, together with the limit $\chi \ll \sigma$ in which our experiments are carried out, is suitable to analyze the ESE decay by the selective excitation of the *A* spin packets within $f(\omega)$.

II. METHODS

A. Theoretical background

To outline our experimental investigation, we consider an inhomogeneous two-level ($S=\frac{1}{2}$) spin system. In a static magnetic field $\mathbf{B}=B_0\hat{z}$ the resonance frequency ω of the spins is distributed as $f(\omega-\omega_0)$ around the center frequency $\omega_0=\gamma B_0$, where γ is the magnetogyric ratio. The echo signal is generated by a sequence of two pulses of a microwave field $\mathbf{b}(t)=2b_1\cos(\omega_1 t)\hat{x}$, lasting t_1 and t_2, respectively, and separated by an interval τ. We denote by $\Delta=\omega_1-\omega_0$ the detuning of the driving field from the center frequency and by $\delta=\omega-\omega_1$ the detuning of the generic spin from the driving field. The first pulse rotates the *A* spins, located within a spectral bandwidth of the order of the Rabi frequency $\chi=\gamma b_1$ about ω_1, by an angle $\theta_1=\beta t_1$, where $\beta=(\chi^2+\delta^2)^{1/2}$, from their initial orientation parallel to $\mathbf{B}$ and induces a transverse magnetization. During the interpulse time τ, the spins dephase owing to the inhomogeneous spreading of ω and the transverse coherence is reversibly lost. When the second pulse rotates these spins by an angle $\theta_2=\beta t_2$, it reverses their precession phases and at a time τ after the second pulse the transverse magnetization is restored giving rise to the emission of the echo signal I_{ESE}. However, the interactions between the spins, occurring in the time interval $t_1+\tau+t_2+\tau$, cause irreversible loss of transversal coherence so that refocussing is not complete. The ESE signal

$I_{ESE}(\tau)$ emitted by the spin system, for fixed values of θ_1 and θ_2, decreases on increasing the interpulse distance τ following a single exponential law

$$I_{ESE}(\tau) = I_0 \exp(-2b\tau), \tag{1}$$

where b expresses the decay rate of the ESE intensity caused by the irreversible dephasing of spins. The role played by ID and SD in the kinetics of the ESE, is taken into account by the following expression of the decay rate:[5,7]

$$b = b_{SD} + b_{ID}\langle \sin^2(\theta_2/2)\rangle_f, \tag{2}$$

where the rate b_{SD} is determined by the SD mechanism whereas b_{ID} is due to the ID effect and it is proportional to the spin concentration C according to[5]

$$b_{ID} = \frac{4\pi^2}{9\sqrt{3}}\gamma^2\hbar C. \tag{3}$$

In Eq. (2) the angular brackets denote the average over the inhomogeneous distribution $f(\omega-\omega_0)$:

$$\langle \sin^2(\theta_2/2)\rangle_f = \int_{-\infty}^{+\infty} \frac{\chi^2}{\delta^2+\chi^2} \sin^2\left(\frac{t_2}{2}\sqrt{\delta^2+\chi^2}\right) f(\delta+\Delta)\,d\delta. \tag{4}$$

So, according to Eq. (4), the coefficient that modulates the ID rate depends on the Rabi frequency χ, on the second pulse lasting time t_2 and on the detuning Δ.

We note that in the Hahn's limit ($\chi \gg \sigma$), the function $f(\delta+\Delta)$ already vanishes when $|\delta| \ll \chi$ and the integral in Eq. (4) reduces to $\sin^2(\theta_{20}/2)$ with $\theta_{20} = \chi \cdot t_2$; i.e., when all the spins are excited, the weight of b_{ID} in Eq. (2) varies between 0 and 1 on varying the second pulse area θ_{20} from 0 to π. In the opposite limit $\chi \ll \sigma$, $f(\delta+\Delta)$ is a function slowly variable with respect to the others and it can be extracted from the integral with the value that assumes at $\delta = 0$, i.e., $\omega = \omega_1$. Then Eq. (4) simplifies to

$$\langle \sin^2(\theta_2/2)\rangle_f \cong f(\Delta) \int_{-\infty}^{+\infty} \frac{\chi^2}{\delta^2+\chi^2} \sin^2\left(\frac{\cdot t_2}{2}\sqrt{\delta^2+\chi^2}\right) d\delta, \tag{5}$$

that is, the average $\langle \sin^2(\theta_2/2)\rangle_f$, at a fixed θ_2 reproduces the resonance line on varying the detuning Δ.

B. Experimental details

Our experiments were carried out in a system of E'_γ centers in vitreous SiO_2.[19] E'_γ centers (unpaired electrons localized on a Si atom) have $S = \frac{1}{2}$. They are particularly suitable for the experiments described here, for their relatively long relaxation times and their narrow and highly inhomogeneous resonance line.[20] These defects were induced by γ irradiating a sample of Infrasil 301, supplied by Heraeus,[21] in a ^{60}Co source at room temperature with total dose of 50 Mrad.[22] The resonance curve of E'_γ centers was obtained by integrating the continuous wave (CW) ESR spectrum detected at room temperature with a Bruker EMX spectrometer. These CW-ESR measurements were performed at 9.8 GHz (X band)

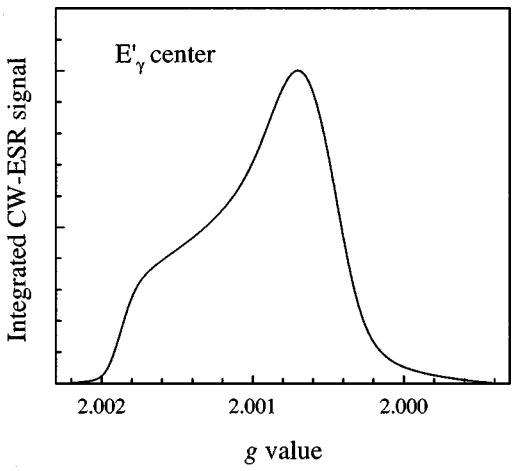

FIG. 1. Integral of the measured ESR signal of E'_γ centers as a function of g values, revealed at 9.8 GHz (X band) in the silica sample I301 irradiated by γ-dose of 50 Mrad.

with a microwave power $P = 800$ nW to avoid saturation and a modulation field with peak-to-peak amplitude $B_m = 0.1$ G at 100 kHz. In Fig. 1, the integrated CW-ESR spectrum of E'_γ centers is shown. As known,[23] it results from axially symmetrical centers, randomly oriented within the amorphous matrix, with main g values $g_\parallel \approx 2.0018$ and $g_\perp \approx 2.0004$.

ESE experiments were carried out at liquid-helium temperature (4.2 K), within the experimental configuration of two photon excitation second harmonic detection, described in previous papers, to which we refer for a thorough discussion on its advantage.[24] In this configuration, we revealed the radiation emitted by the sample, at second harmonic (5.8 GHz) with respect to the incident radiation frequency (2.9 GHz) of the driving field. The Rabi frequency χ was regulated by adjusting the amplitude of the microwave field acting on the sample and determined by revealing the oscillations of the nutational regime excited at the same power level. The measurements reported below were taken at $\chi = 2\pi \times 200$ kHz and $\chi = 2\pi \times 120$ kHz.

Time-decay curves and field-swept ESE spectra were detected by measuring the echo amplitude as a function of the interpulse distance τ at a fixed field and as a function of the static magnetic field B at fixed values of the input pulse sequence, respectively. The pulse sequence was controlled by a programmable pulse generator with a time resolution of 0.01 μs. The signal $I_{ESE}(\tau)$ was detected by a superheterodyne receiver, working at the intermediate frequency of 30 MHz. The video signal output by the receiver, calibrated in dB with the accuracy of ± 0.5 dB, was acquired by a transient recorder and averaged over a number of successive acquisitions, typically 64, for improving the signal-to-noise ratio.

The longitudinal relaxation time T_1 was previously measured in our work conditions ($T = 4.2$ K) by the saturation recovery method. Its value ($T_1 = 0.9 \pm 0.2$ s) determined the repetition frequency ν used in echo experiments: indeed, the condition $\nu \cdot T_1 \ll 1$ must be fulfilled to allow complete thermal relaxation between successive sequences.

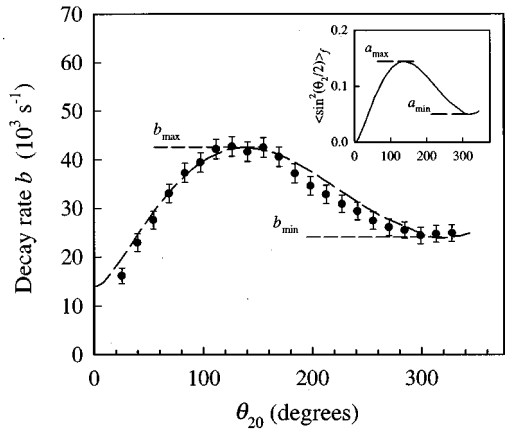

FIG. 2. Echo decay rate b as a function of the second pulse area θ_{20}. Dots are the experimental values of b; the dashed line plots the function defined in Eq. (2), as described in the text. In the inset, the theoretical curve $\langle \sin^2(\theta_2/2)\rangle_f$ is drawn.

III. RESULTS

In order to check the interplay between SD and ID, we investigated the decay of the echo signal intensity as a function of the second pulse area θ_{20}. These measurements were performed using different pulse sequences, all with $\theta_{10}=120°$, and with second pulse area varied in the range from 25° up to 330°.

In the whole range of θ_{20} investigated the experimental data $I_{ESE}(\tau)$ were well fitted by a single exponential law over a dynamic range of at least 10 dB, as expected from Eq. (1). The decay rate could be measured with a typical accuracy of ±5% and was found to depend strongly on θ_{20}. The experimental results are reported in Fig. 2, for $\chi=2\pi\times 200\,\text{kHz}$. As shown, b has a maximum $b_{max}=(43\pm 2)\times 10^3\,\text{s}^{-1}$ at $\theta_{20}\approx 115°$ and a minimum $b_{min}=(24\pm 2)\times 10^3\,\text{s}^{-1}$ at $\theta_{20}\approx 300°$. In the inset of the same figure we report the theoretical dependence of $\langle \sin^2(\theta_2/2)\rangle_f$ on θ_{20} as calculated by numerical integration of Eq. (4) and using the experimental values of χ and $f(\delta+\Delta)$: this curve was used to determine the corresponding extreme values $a_{max}=0.144$ and $a_{min}=0.050$. By comparing the excursion $(b_{max}-b_{min})$ to the theoretical one $(a_{max}-a_{min})$, we inferred the value of $b_{ID}=(b_{max}-b_{min})/(a_{max}-a_{min})=(2.0\pm 0.3)\times 10^5\,\text{s}^{-1}$. Finally, we determined b_{SD} as $b_{SD}=b_{max}-b_{ID}\cdot a_{max}$ and we get $b_{SD}=(1.3\pm 0.3)\times 10^4\,\text{s}^{-1}$. The obtained values of b_{ID} and b_{SD} confirm that the ID is the dominant mechanism of spin-echo decay in our spin system, at least by one order of magnitude. The theoretical curve [Eq. (2)], obtained by substituting these values of b_{SD} and b_{ID}, is drawn in the same figure and evidences the good agreement with our experimental data. By the way, from the obtained value of b_{ID} and from Eq. (3), we are able to estimate the concentration of E'_γ centers in our sample: $C=(2.5\pm 0.3)\times 10^{17}$ spins cm^{-3}. This value agrees reasonably with the one ($C\sim 10^{17}$spins cm^{-3}) obtained by comparison with the CW-ESR signal of a reference ruby (Cr^{3+}:Al_2O_3) sample.

To further characterize the ID mechanism, we investigated how different spin packets, located within the inhomogeneous distribution $f(\omega-\omega_0)$, contribute to the ESE decay. In this second set of experiments, the exciting pulse sequence was kept fixed ($\theta_{10}=\theta_{20}=120°$), while sweeping the magnetic field over the resonance line. Measurements were taken at various values of the interpulse distance τ. The experimental field-swept spectra, obtained for $\chi=2\pi\times 120\,\text{kHz}$ and at various values of τ are reported in Fig. 3. As shown, the profile $I_{ESE}(B)$ changes its shape on varying τ, for $\tau=3\,\mu$s it is a bell-shaped curve, quite similar to the resonance curve of E'_γ centers, whereas, on increasing τ, the central part of the curve decays faster than the wings and, after nearly 45 μs, a dip appears in the $I_{ESE}(B)$ spectrum.

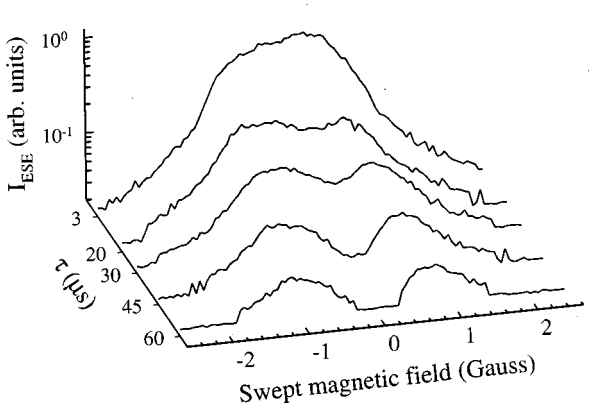

FIG. 3. Field-swept ESE spectra induced by different sequences 120°-τ-120°: $\tau=3\,\mu$s, $\tau=20\,\mu$s, $\tau=30\,\mu$s: $\tau=45\,\mu$s: $\tau=60\,\mu$s.

The dependence of the decay rate on the spectral position of the echo-active A spins was evidenced by looking at the ESE decay ensuing the same 120°-120° pulse sequence for different values of B, i.e., of the detuning Δ. Typical decay curves are shown in Fig. 4 for three values of the detuning $\Delta B=\Delta/\gamma$ from the static magnetic field B_0 at which the bell-shaped curve $I_{ESE}(B)$ has a maximum (see the curve obtained at $\tau=3\,\mu$s in Fig. 3): $\Delta B=0$ G, $\Delta B=+0.5$ G, and

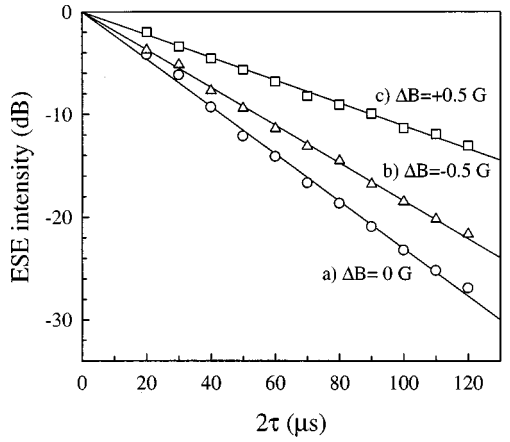

FIG. 4. Experimental echo decay curves, excited by the same two pulse sequence ($\theta_{10}=\theta_{20}=120°$), at three different values of the detuning ΔB from the resonance condition: $\Delta B=0$ G in (a), $\Delta B=-0.5$ G in (b), and $\Delta B=+0.5$ G in (c). The continuous lines plot the single-exponential functions $I_{ESE}(\tau)=I_0\exp(-2b\tau)$ that best fit the experimental points.

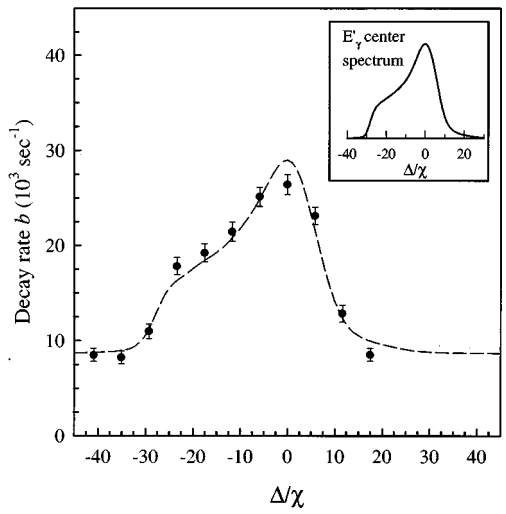

FIG. 5. The echo decay rate b, measured as a function of detuning Δ, expressed in unit of the Rabi frequency χ. The dashed line plots the best-fitting function defined in Eq. (2) in which $\langle \sin^2(\theta_2/2)\rangle_f$ is evaluated as described in the text. In the inset it is shown the integral of the CW-ESR spectrum of E'_γ centers.

$\Delta B = -0.5$ G. All the curves are well-fitted by single exponential decay laws expressed by Eq. (1), $I_{\mathrm{ESE}}(\tau) = I_0 \exp(-2b\tau)$, but for the different values of the rate, which is faster at the resonance $\Delta B = 0$ G [$b = (26 \pm 1) \times 10^3\ \mathrm{s}^{-1}$] and slower on both sides $b = (21 \pm 1) \times 10^3\ \mathrm{s}^{-1}$ at $\Delta B = -0.5$ G and $b = (12.8 \pm 0.5) \times 10^3\ \mathrm{s}^{-1}$ at $\Delta B = +0.5$ G.

The different decay kinetics which affects the inhomogeneous distribution of spin packets is evidenced in Fig. 5 where we report the measured decay rate b as a function of the detuning Δ of the driving field from the peak value of $f(\omega - \omega_0)$, in units of χ. The decay rate is maximum for $\Delta/\chi = 0$ (i.e., for the spin packets located at the peak of the distribution of E'_γ centers) and decreases on increasing $|\Delta/\chi|$. In the same figure it is drawn the curve described by Eq. (2) in which the function $\langle \sin^2(\theta_2/2)\rangle_f$ was numerically evaluated by using the experimental values of the parameters $\chi = 2\pi \times 120$ kHz and $\theta_{20} = 120°$, while b_{SD} and b_{ID} were obtained by a best-fitting procedure. In this case we get $b_{\mathrm{SD}} \approx (0.9 \pm 0.3) \times 10^4\ \mathrm{s}^{-1}$ and $b_{\mathrm{ID}} \approx (2.3 \pm 0.3) \times 10^5\ \mathrm{s}^{-1}$ respectively, i.e., in agreement with the values above reported (Fig. 2) within the experimental uncertainty of our measurements. We note that the envelope of experimental points on varying the detuning is quite similar to the shape of the CW-ESR spectrum of E'_γ centers, also displayed in the inset of Fig. 5 in the scale Δ/χ, apart from the vertical shift due to the SD contribution.

IV. DISCUSSION

Our experimental investigation, carried out in a highly inhomogeneous spin system (E'_γ centers in glassy silica), allowed us to evidence two distinguishable contributions to the irreversible spin dephasing which causes the attenuation of the echo signal generated by a two-pulse sequence. These two relaxation mechanisms, recognized as SD and ID processes, were quantitatively determined by measuring the echo decay rate b at various values of the second pulse area θ_{20} (Fig. 2). In particular, we found that the ID effect is the main contribution to the ESE decay for the E'_γ centers, present in the investigated sample with a concentration of $\sim 2.5 \times 10^{17}\ \mathrm{cm}^{-3}$. This study adds to previous experimental observations obtained for other spin systems,[2,5–8,10,11,25] and confirms the validity of the theoretical model based on Eqs. (2) and (4) describing the interplay between SD and ID and the dependence of the latter on the second pulse area θ_{20}.

New aspects of the ID effect were evidenced both by the field-swept echo profiles and by the dependence of b on the detuning Δ of the driving field from the peak value of the resonance line. Our experiments clearly show the different decay kinetics of the ESE signal generated by the A spins excited at distinct spectral positions. These features could be taken into account by Eq. (2), according to which the dependence of the decay rate b on the detuning Δ (Fig. 5) results from two contributions: a constant term, due to the SD, and a term related to the ID process whose weight depends on the detuning Δ via the function $\langle \sin^2(\theta_2/2)\rangle_f$. Moreover, this analysis allows us to interpret the similarity of this curve with the CW-ESR spectrum of E'_γ centers. In fact, as derived in Eq. (5), in the limit $\chi \ll \sigma$, in which our experiments were carried out, the function $\langle \sin^2(\theta_2/2)\rangle_f$ is proportional to $f(\Delta)$ so that the ID rate dependence on Δ reproduces the shape of the E'_γ centers resonance line. It is worth noting that the agreement between our results and Eq. (5) confirms that the ID effectiveness is closely related to the concentration of echo-active spins and so it scales following their spectral distribution.

At the same time, the different extent of ID rate on varying the spectral position of the excited A spins is the cause of changes on the shape of echo field-swept profiles observed in our experiments when the time interval τ between the microwave pulses is increased. Indeed, during the second pulse in which ID is effective, the spin packets localized within χ around the frequency ω_0 lose their coherence more rapidly than those detuned from ω_0 so causing a dip in the center part of the echo profile at long values of the interpulse τ.

V. CONCLUSIONS

In conclusion, we have reported a detailed investigation on the echo generation of a spin system consisting in E'_γ centers in silica in which the ID is the main relaxation process. The selective excitation of spin packets within the inhomogeneous resonance line allowed us to evidence the different extent of the ID dephasing rate on varying the spectral position of the echo-active spins. This effect induces changes in the field-swept echo spectra detected at different inter pulses intervals. Moreover, we found that the dependence of the ID decay rate on the detuning from the central frequency reproduces the shape of the ESR absorption. Our results confirm the existing theory on the echo-decay dynamics in solid spin system.

The spectral related features of ID are particularly rel-

evant for its connection with the interpretation of experiments based on field-swept echo measurements to distinguish spin species with different transversal relaxation times T_2 overlapping in the CW-ESR spectrum. This distinction would be prevented owing to the ID effect of single spin species, as evidenced in the present work and also suggested in previous papers for experiments performed on glassy states in biological objects.[26]

ACKNOWLEDGMENTS

The authors thank Professor E. Calderaro for taking care of sample irradiation in the γ-irradiator IGS-3 of Department of Nuclear Engineering of Palermo and are grateful to G. Lapis for technical assistance. Partial financial support has been given by the Italian Ministry for University and Scientific Research.

*Corresponding author. Email address: cannas@fisica.unipa.it

[1] W. B. Mims, in *Electron Paramagnetic Resonance*, edited by S. Geshwind (Plenum, New York, 1972), pp. 263–351.
[2] K. M. Salhikov and Y. D. Tsevetkov, in *Time Domain Electron Spin Resonance*, edited by L. Kevan and R. N. Schwartz (Wiley, New York, 1979), pp. 231–277.
[3] A. Ponti and A. Schweiger, Appl. Magn. Reson. **7**, 363 (1994).
[4] D. A. Bozanic, D. Mergerian, and R. W. Minarik, Phys. Rev. Lett. **21**, 541 (1968).
[5] A. M. Raitzmiring, K. M. Salikhov, B. A. Umanskii, and Y. D. Tsvetkov, Sov. Phys. Solid State **16**, 492 (1974).
[6] A. M. Raitzmiring, K. M. Salikhov, S. F. Bychkov, and Y. D. Tsvetkov, Sov. Phys. Solid State **17**, 303 (1975).
[7] K. M. Salikhov, S. A. Dzuba, and A. M. Raitsmiring, J. Magn. Reson. **42**, 255 (1981).
[8] V. I. Dudkin, V. Y. Petrun'kin, S. V. Rubinov, and L. I. Uspenskil, Sov. Phys. Solid State **28**, 729 (1986).
[9] V. A. Atsarkin, Magn. Reson. Rev. **16**, 1 (1991).
[10] V. V. Kurshev and T. Ichikawa, J. Magn. Reson. **96**, 563 (1992).
[11] R. Boscaino and F. M. Gelardi, Phys. Rev. B **46**, 14 550 (1992).
[12] B. Herzog and E. L. Hahn, Phys. Rev. **103**, 148 (1956).
[13] R. Boscaino, F. M. Gelardi, and M. Cannas, Phys. Rev. B **53**, 302 (1996).
[14] J. R. Klauder and P. W. Anderson, Phys. Rev. **125**, 912 (1962).
[15] P. Hu and L. R. Walker, Phys. Rev. B **18**, 1300 (1978).
[16] M. Romanelli and L. Kevan, J. Magn. Reson. **91**, 549 (1991).
[17] M. Romanelli and L. Kevan, Concepts Magn. Reson. **9**, 403 (1997).
[18] M. Brustolon, A. Zoleo, and A. Lund, J. Magn. Reson. **137**, 389 (1999).
[19] R. A. Weeks, J. Appl. Phys. **27**, 1376 (1956); D. L. Griscom, Nucl. Instrum. Methods Phys. Res. B **1**, 481 (1984).
[20] S. Agnello, R. Boscaino, M. Cannas, F. M. Gelardi, and R. Shakhmuratov, Phys. Rev. A **59**, 4087 (1999).
[21] Heraeus Quartzglass, Hanau, Germany, catalogue POL-0/102/E.
[22] S. Agnello, R. Boscaino, M. Cannas, and F. M. Gelardi, Appl. Magn. Reson. **19**, 363 (2000).
[23] D. L. Griscom, E. J. Friebele, and G. H. Siegel, Jr., Solid State Commun. **15**, 479 (1974).
[24] R. Boscaino, F. M. Gelardi, and J. P. Korb, Phys. Rev. B **48**, 7077 (1993).
[25] I. N. Kurkin and V. I. Shlenkin, Sov. Phys. Solid State **21**, 847 (1979).
[26] S. A. Dzuba, Y. A. Golovina, and Y. D. Tsvetkov, J. Magn. Reson., Ser. B **101**, 134 (1993).